The plasma physics of cosmic rays in star-forming regions

M. Padovani[1,2], A. Marcowith[1], P. Hennebelle[3], K. Ferrière[4]

[1] Laboratoire Univers et Particules de Montpellier, Université de Montpellier, France

E-mail: [Marco.Padovani,Alexandre.Marcowith]@umontpellier.fr

[2] INAF–Osservatorio Astrofisico di Arcetri, Firenze, Italy

[3] CEA, IRFU, SAp, Centre de Saclay, Gif-Sur-Yvette, France

E-mail: Patrick.Hennebelle@cea.fr

[4] IRAP, Université de Toulouse, France

E-mail: Katia.Ferriere@irap.omp.eu

Abstract. It is largely accepted that Galactic cosmic rays, which pervade the interstellar medium, originate by means of shock waves in supernova remnants. Cosmic rays activate the rich chemistry that is observed in a molecular cloud and they also regulate its collapse timescale, determining the efficiency of star and planet formation, but they cannot penetrate up to the densest part of a molecular cloud, where the formation of stars is expected, because of energy loss processes and magnetic field deflections. Recently, observations towards young protostellar systems showed a surprisingly high value of the ionisation rate, the main indicator of the presence of cosmic rays in molecular cloud. Synchrotron emission, the typical feature of relativistic electrons, has been also detected towards the bow shock of a T Tauri star. Nevertheless, the origin of these signatures peculiar to accelerated particles is still puzzling. Here we show that particle acceleration can be driven by shock waves occurring in protostars through the **first-order Fermi acceleration mechanism.** We expect that shocks in protostellar jets can be efficient accelerators of protons, which can be boosted up to **mildly** relativistic energies. **A strong acceleration can also take place at the protostellar surface, where shocks produced by infalling material during the phase of collapse are powerful enough to accelerate protons. Our model shows that thermal particles can experience an acceleration during the first phases of a system similar to the proto-Sun and can also be used to explain recent observations.** The presence of a local source of cosmic rays may have an unexpected impact over the process of formation of stars and planets as well as on the pre-biotic molecule formation.

Keywords: Cosmic Rays, Interstellar Medium: Jets and Outflows, Stars: Protostars.

1. Introduction

The evolutionary path of a molecular cloud can be described by observations at different scales: from diffuse clouds, to dense prestellar cores, to protostellar systems. There is a

key component whose presence, or absence, turns out to be crucial for all the physical and chemical processes: cosmic rays (hereafter CRs). Mainly constituted by protons and heavy nuclei accelerated in Galactic supernova remnants or in other very energetic sources, CRs with energy below GeV cause most of the ionisation **(see, e.g., Grenier *et al* [20])**. In particular, from the ionisation of molecular hydrogen, H_3^+ is rapidly formed:

$$\begin{aligned} &CR + H_2 \rightarrow H_2^+ + e + CR' \\ &H_2^+ + H_2 \rightarrow H_3^+ + H\,. \end{aligned}$$

H_3^+ is a pivotal molecule leading to the formation of carbon- and nitrogen-bearing molecular ions that are commonly observed in star-forming regions such as HCO^+, N_2H^+, H_3O^+, and OH^+ through the following reactions

$$\begin{aligned} H_3^+ + CO &\rightarrow HCO^+ + H_2 \\ H_3^+ + N_2 &\rightarrow N_2H^+ + H_2 \\ H_3^+ + H_2O &\rightarrow H_3O^+ + H \\ H_3^+ + O &\rightarrow OH^+ + H_2\,. \end{aligned}$$

Molecular ions are then destroyed by electronic recombination bringing to the formation of crucial molecules such as ammonia (NH_3) and formaldehyde (H_2CO). Finally, slower neutral-neutral reactions create species such as hydrogen cyanide ($CH_2 + N \rightarrow HCN + H$), a critical molecule for the synthesis of amino acids and DNA nucleotides (e.g. Ferris *et al* [16]). Looking at this simplified reaction network backwards, summarised in figure 1, it is clear that CRs activate the complex chemistry that is observed at infrared and radio wavelengths, also affecting the genesis of pre-biotic molecules.

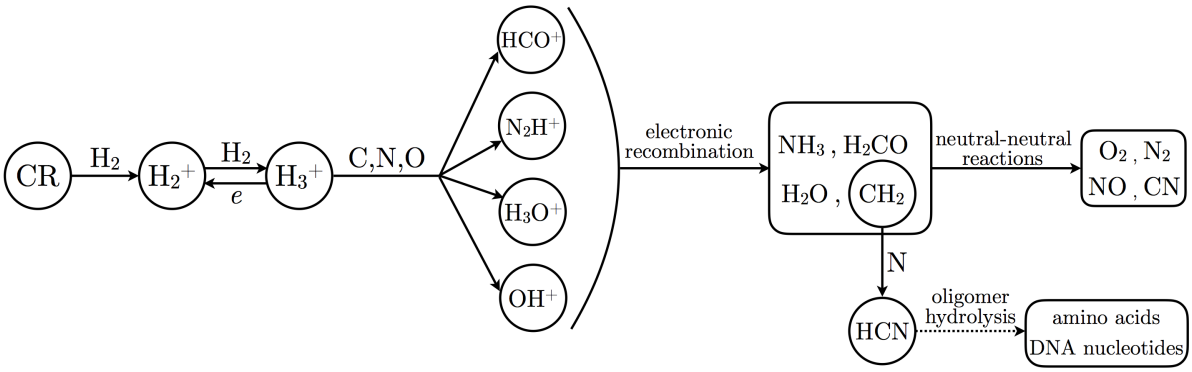

Figure 1. Complex chemistry originated by CRs in molecular clouds. This sketch represents only some of the main species created by CR ionisation.

By determining the ionisation fraction, CRs additionally set the degree of coupling between local magnetic field and gas. In fact, while neutrals can drift towards the centre of a collapsing dense molecular cloud core, charged particles are frozen into the magnetic

field lines. As a consequence a frictional force creates a coupling between neutrals and charged particles. The higher the ionisation rate, the higher the number of charges, and the stronger the ion-neutral coupling. In this sense, CRs are responsible for the collapse time of a molecular cloud as well as for the efficiency of star formation (Shu *et al* [41]; Padovani *et al* [31, 32]).

Part of the kinetic energy of CRs entering a molecular cloud is transformed into heating. In fact, CRs with energy lower than the ionisation potential of molecular hydrogen (15.4 eV) heat the gas from the dissociation of its triplet state, from the de-excitation of its rovibrational levels, and from the reactions driven by primary CRs (a process known as chemical heating; Glassgold *et al* [19]). Thus CRs play an important role in the thermal balance of a cloud, determining the gas temperature in particular density intervals (Galli and Padovani [17]).

Collisions between CRs and molecular hydrogen can also excite H_2 in the Lyman ($X^1\Sigma_g^+ \rightarrow B^1\Sigma_u^+$) and Werner ($X^1\Sigma_g^+ \rightarrow C^1\Pi_u$) states. The almost instantaneous de-excitation which follows is accompanied by the emission of UV photons (Prasad and Tarafdar [37]). This process determines the charge distribution on dust grains (Cecchi-Pestellini and Aiello [9]; Ivlev *et al* [22]). In fact, while in absence of CRs grains are mainly negatively charged because of the high collision rate with thermal electrons‡, CR-generated UV photons remove electrons from grains through photoelectric effect, creating a population of positively charged grains. This process leads to the generation of large dust aggregates that is essential for the formation of planetesimals.

In addition to these main aspects, CRs with higher energy (GeV-TeV) contribute to the γ emission observed in molecular clouds through pion production. Finally, except for ^{7}Li, isotopes of Li, Be, and B are uniquely created by $\sim$ 100 MeV CRs through spallation reactions.

The presence of CRs can be indirectly proved by observing molecular species such as H_3^+, OH^+, and H_2O^+ in diffuse clouds (e.g., Indriolo *et al* [21]; Neufeld *et al* [27]); CO, HCO^+ and DCO^+ in prestellar cores (e.g., Caselli *et al* [7]) **and in molecular clouds close to supernova remnants (e.g., Vaupré *et al* [45])**; HCO^+ and N_2H^+ in protostellar regions (e.g., Ceccarelli *et al* [8]). By observing these molecular transitions it is possible to compute the CR ionisation rate, ζ, namely the number of ionisation of hydrogen molecules per unit time. The CR ionisation rate is the key-brick parameter in chemical codes to interpret the abundance of the observed molecular lines as well as in non-ideal magnetohydrodynamic simulations to study the collapse of molecular clouds and the star formation. This rate spans over a few orders of magnitude: from $10^{-15} - 10^{-16}$ s^{-1} in diffuse regions to $10^{-17} - 10^{-18}$ s^{-1} in prestellar cores, while in protostars one expects even lower values ($\zeta \lesssim 10^{-19}$ s^{-1}) whose minimum is fixed by the ionisation of radioactive nuclei (Umebayashi and Nakano [44]). The decrease of ζ with increasing H_2 density is due to the attenuation of the CR flux because of energy

‡ The thermal speed of ions is a factor $\sqrt{m_i/m_e}$ smaller than that of electrons, so ion-grain collisions are far more rare.

loss processes (Padovani *et al* [28]; Padovani and Galli [30]) and mirroring and focusing effects due to the presence of magnetic fields (Desch *et al* [12]; Padovani and Galli [29]; Padovani *et al* [31]).

However, using the Herschel telescope, high-ionisation rates have been recently estimated in Class 0/I protostars (Ceccarelli *et al* [8]; Podio *et al* [35]). Besides, the Giant Metrewave Radio Telescope and the Expanded Very Large Array detected synchrotron emission in the bow shock of the T Tauri star DG Tau (Ainsworth *et al* [2]), a clue for the presence of relativistic electrons. Both high values of ζ and synchrotron emission cannot be explained by the interstellar flux of CRs because it is strongly attenuated at these high densities. Here we suggest the possibility of accelerating CRs in the shocks present in protostellar jets as well as on the protostellar surface.

2. Energetics

Before studying any possible acceleration mechanism inside or close to a protostar, we have to verify that some potential energy is available to be converted into particle kinetic energy. The gravitational luminosity of a shock caused by accretion on the surface of a protostar is given by

$$L_{\rm gr} = \frac{GM\dot{M}}{R_{\rm sh}}\,, \tag{1}$$

where G is the gravitational constant, M is the mass of the protostar, $\dot{M}$ is the rate of accretion, and $R_{\rm sh}$ is the radius of the shock. If we consider the collapse of an accreting envelope onto a protostar (also known as Class 0 phase), then we can assume $M = 0.1\ M_\odot$, $\dot{M} = 10^{-5}\ M_\odot\ {\rm yr}^{-1}$, and $R_{\rm sh} = 2 \times 10^{-2}$ AU (Shu *et al* [40]; Masunaga and Inutsuka [25]), obtaining $L_{\rm gr} = 3 \times 10^{34}$ erg s^{-1}.

The luminosity due to the interstellar flux of CRs impacting a dense core in a molecular cloud can be computed by

$$L_{\rm CR} = R_{\rm c}^2 V_{\rm A} \epsilon_{\rm CR}\,, \tag{2}$$

where $R_{\rm c}$ is the radius of the dense core and $V_{\rm A}$ is the Alfvén speed of the local medium. The energy density of the interstellar CRs, $\epsilon_{\rm CR}$, is defined by

$$\epsilon_{\rm CR} = 4\pi \int_0^\infty \frac{E j(E)}{v(E)} {\rm d}E\,, \tag{3}$$

where $j(E)$ is the differential CR flux, namely the number of CRs per unit area, time, solid angle, and energy, and v is the CR velocity. Adopting the typical value for the radius of a dense molecular cloud core, $R_{\rm c} = 0.1$ pc, surrounded by a warm neutral medium with total hydrogen density $n_{\rm H} = 0.5$ cm^{-3} and a magnetic field strength $B = 3\ \mu$G (Ferrière [15]), and $\epsilon_{\rm CR} = 1.3 \times 10^{-12}$ erg cm^{-3} based on the most recent observations of Voyager 1 (Stone *et al* [42]), then $L_{\rm CR} = 1.2 \times 10^{29}$ erg cm$^{-3} \ll L_{\rm gr}$. From previous studies, we know that the flux of interstellar CRs is weakened during the propagation in a molecular cloud (section 1) so that $\epsilon_{\rm CR}$ is expected to be even lower and $L_{\rm gr} \ggg L_{\rm CR}$ getting closer to the protostar.

This simple estimate demonstrates that a small fraction of gravitational energy can be converted into acceleration of local thermal particles whose luminosity can prevail over the interstellar CR luminosity. In this work we refer to low-mass protostar, but massive stars have even larger gravitational energy since $\dot{M}$ increases up to $10^{-3}\ M_\odot\ \mathrm{yr}^{-1}$. Thus, in principle, local thermal particles can be more easily accelerated to higher energies so that it can be possible to observe their γ emission. (e.g., **Tavani** *et al* **[43]; Abdo** *et al* **[1]**; Araudo *et al* [3]; Bosch-Ramon *et al* [6]; Munar-Adrover *et al* [26]).

3. Particle acceleration in protostars

A number of mechanisms can be responsible for the acceleration of particles when shocks are present: turbulent second-order Fermi acceleration (Prantzos *et al* [36]), shear acceleration at the interface between the jet and the outflow of a protostar (Rieger and Duffy [38]), acceleration by shocked background turbulence (Giacalone and Jokipii [18]), and acceleration in magnetic reconnection sites (De Gouveia Dal Pino and Lazarian [11]).

In this paper we concentrate on the first-order Fermi acceleration mechanism, also known as diffusive shock acceleration (hereafter DSA), as proposed in Padovani *et al* [33, 34]. According to DSA, charged particles gain energy each time that they cross a shock, but an efficient acceleration takes place only if fluctuations of the magnetic field are present around the shock. In fact, these fluctuations guarantee the scattering of the pitch angle so that particles can cross the shock front many times, easily reaching relativistic energies, until they escape in the downstream medium (see e.g., Drury [13]; Kirk [23]). In this sense DSA can "transform" local thermal particles of a protostellar system into cosmic rays. In the following we only discuss the acceleration of thermal protons. In fact, as pointed out in Padovani *et al* [33, 34], thermal electrons can also be accelerated, but they are soon thermalised because of energy losses and wave damping.

3.1. Ion-neutral damping

DSA is a well-studied process that takes place in supernova remnants. However, in protostars the medium is not fully ionised and the friction between ions and neutral particles can strongly quench the DSA. If neutrals and ions are coupled, namely if they move coherently, then the waves generated by ions are weakly damped and particles can be efficiently accelerated. The wave damping rate, Γ, is given by Drury *et al* [14]

$$\Gamma = \frac{\omega^2}{\omega^2 + \omega_i^2}\omega_n\,, \tag{4}$$

where $\omega_i = n_\mathrm{H} x \langle\sigma v\rangle$ and $\omega_n = n_\mathrm{H}(1-x)\langle\sigma v\rangle$ are the ion and neutral pulsation, respectively; σ is **the sum of charge exchange and elastic cross sections**, v the collision velocity, and the mean value of their product is given by Kulsrud and Cesarsky [24]

$$\langle\sigma v\rangle \approx 8.4\times10^{-9} T_4^{0.4}\ \mathrm{cm}^3\ \mathrm{s}^{-1}\,, \tag{5}$$

with T_4 the temperature in unit of 10^4 K. Equation (5) is valid for temperatures in the range 10^2 K to 10^5 K. The ionisation fraction, x, is defined as the ratio between the ion density, n_i, and the total hydrogen density (neutrals plus ions), $n_{\rm H} = n_n + n_i$. The resonant wave pulsation fulfils the condition $\omega \sim V_{\rm A}/r_{\rm g} \propto E^{-1}$, where $V_{\rm A}$ is the Alfvén speed of the total gas, $r_{\rm g}$ the gyroradius, and E the kinetic energy of the particle. Neutrals and ions are coupled if the wave pulsation is smaller than the momentum transfer rate from ions to neutrals, namely when $\omega < \omega_i$. In this regime $\Gamma \propto \omega^2 \propto E^{-2}$, so the wave damping decreases for larger energies. Figure 2 shows the wave damping rate as a function of the wave pulsation. The condition $\omega = \omega_i$ provides the energy that separates the coupled and decoupled regime, $E_{\rm coup}$, by solving

$$\gamma\beta = 8.8 \times 10^{-5} T_4^{0.4} (n_6 x)^{-1.5} B_{-5}^2 \,, \tag{6}$$

where γ is the Lorentz factor, $\beta = \gamma^{-1}\sqrt{\gamma^2 - 1}$, n_6 is the total hydrogen density in unit of 10^6 cm^{-3}, and B_{-5} is the magnetic field strength in unit of 10 μG.

The upper energy limit due to the damping of the waves, $E_{\rm damp}$, is found by equating the local CR flux advected downstream by the flow to the flux lost upstream due to the damping of waves confining the particles. Following Drury *et al* [14] (see also Appendix D in Padovani *et al* [34]), $E_{\rm damp}$ is computed from

$$\begin{aligned} \gamma\beta^2 = 8.8 \times 10^{-5} \Xi U_2^3 T_4^{-0.4} n_6^{-0.5} \times \\ (1-x)^{-1} B_{-5}^{-4} \widetilde{P}_{-2} \,, \end{aligned} \tag{7}$$

where

$$\Xi = B_{-5}^4 + 1.4 \times 10^{12} \gamma^2 \beta^2 T_4^{0.8} n_6^3 x^2 \,, \tag{8}$$

with U_2 the upstream velocity of the flow in the frame of reference of the shock in unit of 100 km s^{-1}, and $\widetilde{P}_{-2}$ the fraction of the ram pressure ($n_{\rm H} m_{\rm p} U^2$) that goes into the acceleration of local CRs in unit of 10^{-2}. Following Berezhko and Ellison [5], $\widetilde{P}$ is proportional to the efficiency of the shock, η, which is the fraction of thermal plasma particles entering the acceleration process, **and it reads**

$$\widetilde{P} = \eta r \left(\frac{c}{U}\right)^2 \widetilde{p}_{\rm inj}^{\,a} \left(\frac{1 - \widetilde{p}_{\rm inj}^{\,b_1}}{2r-5} + \frac{\widetilde{p}_{\rm max}^{\,b_2} - 1}{r-4} \right) , \tag{9}$$

where $a = 3/(r-1)$**,** $b_1 = (2r-5)/(r-1)$**,** $b_2 = (r-4)/(r-1)$**, and** $\widetilde{p}_k = p_k/(m_p c)$ **is the normalised momentum. Subscripts** $k = {\rm inj}, {\rm max}$ **refer to the injection (or minimum) momentum of a particle able to cross the shock that enters the process of acceleration, and the maximum momentum reached by an accelerated particle, respectively.** While in supernova remnants it is assumed $\widetilde{P} \approx 10\%$, protostars are much less energetic sources and one expects $\widetilde{P} \ll 10\%$. These values of $\widetilde{P}$ give $\eta \in [10^{-6}, 10^{-5}]$. When $E_{\rm damp} > E_{\rm coup}$, ion and neutrals are coupled and DSA can efficiently work.

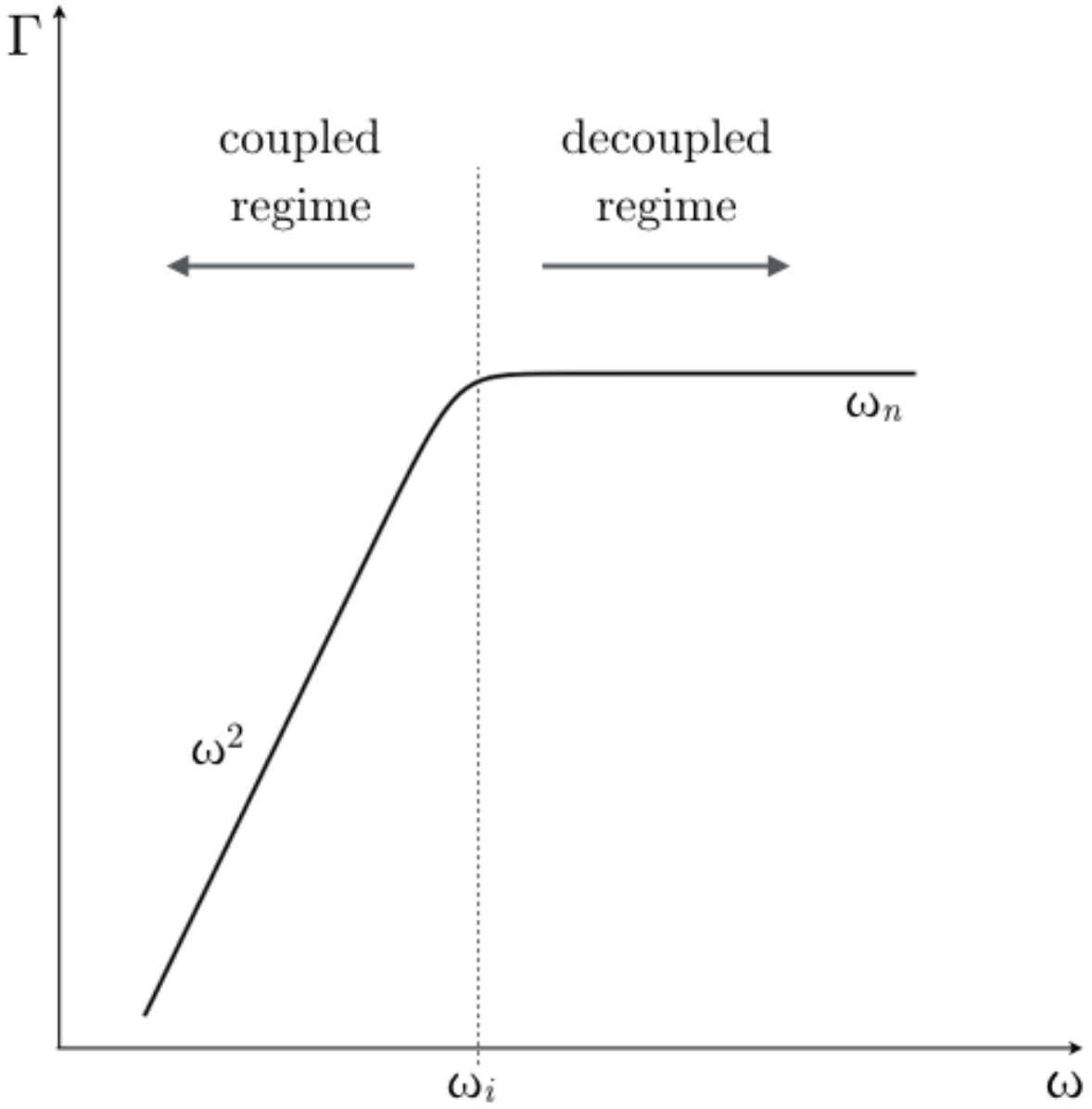

Figure 2. Wave damping rate as a function of wave pulsation. The *dashed vertical line* separates the regime where ions and neutrals are coupled ($\Gamma \propto \omega^2$) or decoupled ($\Gamma \propto \omega_n$).

3.2. Timescales

In this section we describe the timescales of all the processes related to the local acceleration of CRs. The acceleration time, $t_{\rm acc}$, has to be shorter than the collision time, $t_{\rm coll}$, namely particles have to be accelerated before they start to lose energy because of collisions. We generalise the equation to compute $t_{\rm acc}$ in Drury *et al* [14] in order to account for both parallel and perpendicular shocks

$$t_{\rm acc} = 2.9(\gamma-1)\frac{r[1+r(k_{\rm d}/k_{\rm u})^{\alpha}]}{k_{\rm u}^{\alpha}(r-1)}U_2^{-2}B_{-5}^{-1}\ {\rm yr}\,, \tag{10}$$

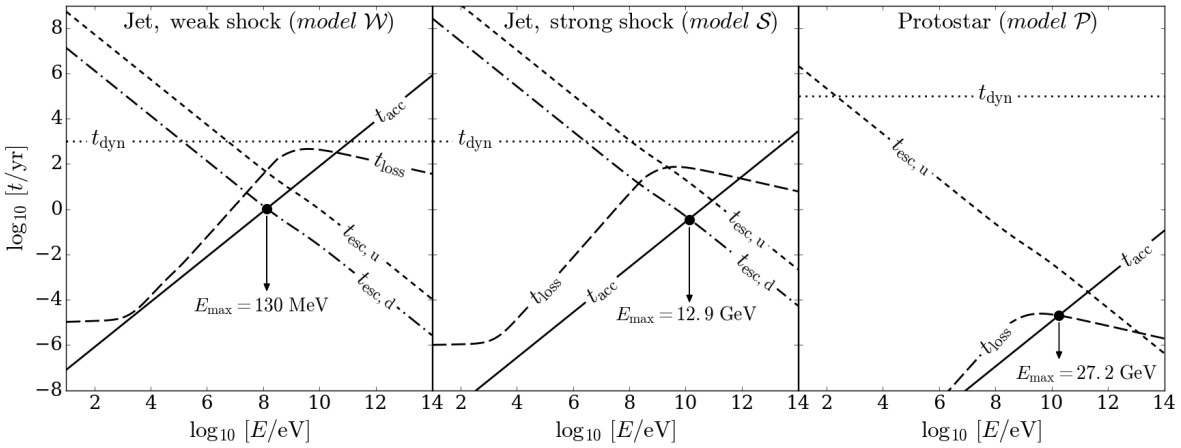

Figure 3. Timescales for the processes described in section 3.2 as a function of the particle kinetic energy for three different shocks (see parameters listed in table 1): a weak and strong shock in the jet (left and middle panel) and a shock on the protostellar surface (right panel). Black solid circles show the solution of equation 18 with the corresponding values of the maximum energy reached by a proton.

where $k_{\rm u,d}$ are the upstream/downstream diffusion coefficient normalised to the Bohm coefficient

$$k_{\rm u} = \left(\frac{\kappa_{\rm u}}{\kappa_{\rm B}}\right)^{-\alpha} = \left(\frac{3eB}{\gamma\beta^2 m_{\rm p} c^3}\kappa_{\rm u}\right)^{-\alpha} \tag{11}$$

with e the elementary charge and r the shock compression ratio. For a perpendicular shock $k_{\rm u} = rk_{\rm d}$ and $\alpha = 1$, while for a parallel shock $k_{\rm u} = k_{\rm d}$ and $\alpha = -1$. The collisional energy loss time reads

$$t_{\rm loss} = 10\frac{\gamma - 1}{\beta} n_6^{-1} L_{-25}\ {\rm yr}\,, \tag{12}$$

where L_{-25} is the energy loss function in unit of 10^{-25} GeV cm^2 (Padovani *et al* [28] and Appendix A in Ivlev *et al* [22]).

Another condition comes from the geometry of the source: acceleration must take place before particles start to escape towards the source (upstream) and in the perpendicular direction (both upstream and downstream). More specifically, the diffusion length in the upstream medium has to be a fraction $\epsilon < 1$ of the distance between the source and the shock, $R_{\rm sh}$, that is $\kappa_{\rm u}/U = \epsilon R_{\rm sh}$. This relation can be translated into a timescale for the upstream particle escape, $t_{\rm esc,u}$, that reads

$$t_{\rm esc,u} = 22.9\frac{k_{\rm u}^{\alpha}}{\gamma\beta^2} B_{-5} R_{\rm sh,2} \mathscr{R}\ {\rm yr}\,, \tag{13}$$

where $R_{\rm sh,2}$ is the shock radius in unit of 100 AU. For a spherical geometry such as in protostellar surface shocks $\mathscr{R} = \epsilon R_{\rm sh,2}$, but in shocks along a jet, local CRs can also escape in the perpendicular direction and in this case $\mathscr{R} = \min(\epsilon R_{\rm sh,2}, R_{\perp,2})$, where $R_{\perp,2}$ is the transverse jet size in unit of 100 AU.

In the case of jet shocks, it is also possible to have particle escape in the downstream medium in the transverse direction. The corresponding timescale§, $t_{\rm esc,d} = R_\perp^2/(4\kappa_{\rm d})$, can be rewritten as

$$t_{\rm esc,d} = 5.7\frac{\mathscr{C}}{\gamma\beta^2}B_{-5}R_{\perp,2}^2 \ {\rm yr}\,, \tag{14}$$

where $\mathscr{C} = r^2$ or 1 for a perpendicular or a parallel shock, respectively.

Finally, there is a further condition due to the shock age: the acceleration time has to be shorter than the dynamical time of the system, $t_{\rm dyn}$, which is of the order or larger than 10^3 yr for a jet shock (de Gouveia dal Pino [10]) and equal to the accretion time, about 10^5 yr, in the case of a protostellar surface shock (Masunaga and Inutsuka [25]).

3.3. Maximum energy at the shock surface

The flow has to be super-Alfvénic and supersonic in order to provide an efficient acceleration, namely

$$U > \max(V_{\rm A}, c_{\rm s})\,, \tag{15}$$

where the Alfvén speed and the ambient sound speed read

$$V_{\rm A} = 2.2\times10^{-2}n_6^{-0.5}B_{-5} \ {\rm km\ s^{-1}} \tag{16}$$

and

$$c_{\rm s} = 9.1[\gamma_{\rm ad}(1+x)T_4]^{0.5} \ {\rm km\ s^{-1}}\,, \tag{17}$$

respectively, and $\gamma_{\rm ad}$ is the adiabatic index. Then, once the condition $E_{\rm damp} > E_{\rm coup}$ is fulfilled (section 3.1), the maximum energy reached by a thermal proton is given by

$$t_{\rm acc} = \min(t_{\rm loss}, t_{\rm esc,u}, t_{\rm esc,d}, t_{\rm dyn})\,. \tag{18}$$

We analyse three acceleration sites in a protostar: shocks in the accreting envelope still present in the early phase of the formation of a protostar, shocks along a jet, and shocks on the surface of a protostar. Shocks in the envelope are not efficient in accelerating particles because shock velocity and ionisation fraction are too small ($U \sim 1-10$ km s^{-1}, $x \lesssim 10^{-6}$) so that $E_{\rm damp} < E_{\rm coup}$ and the magnetic field strength is high enough ($B \sim 1-100$ mG) to generate sub-Alfvénic shocks, then equation (15) is not verified.

Values of shock velocity, magnetic field strength, total hydrogen density, ionisation fraction, temperature, and shock radius for jet and surface shocks can be estimated from observations as well as with the aid of numerical simulations. We consider two extreme cases for jets, a weak and a strong shock (labelled "model $\mathcal{W}$" and "model $\mathcal{S}$", respectively) and the case of a shock on a protostellar surface described in Masunaga and Inutsuka [25] (labelled "model $\mathcal{P}$"). Table 1 lists the values of the parameters.

§ The factor 4 in the denominator accounts for the fact that the downstream diffusion in the transverse direction is in two dimensions.

The upstream diffusion coefficient can be written as (Drury [13])

$$k_u = \left(\frac{\kappa_{\rm u}}{\kappa_{\rm B}}\right)^{-\alpha} = \left(\frac{B}{\delta B}\right)^2 . \tag{19}$$

In the following we assume $k_{\rm u} = 1$, namely the Bohm regime, $\kappa_{\rm u} = \kappa_{\rm B}$. This also means that the fluctuations of the magnetic field, responsible for the scattering of the pitch angle of the particles, get their maximum value ($\delta B = B$) and in this case DSA is very effective. **In Padovani *et al* [34] we discussed the case of departure from the Bohm regime.** We also fix $\eta = 10^{-5}$ which fulfils the condition $\widetilde{P} \lesssim 1\%$ (see also Padovani *et al* [34]).

Figure 3 shows the maximum energy reached by a proton. We find $E_{\rm max} =$ 0.13 GeV, 12.9 GeV, and 27.2 GeV for the model $\mathcal{W}$, $\mathcal{S}$, and $\mathcal{P}$, respectively. Also electrons can be accelerated up to 0.3 GeV, but for a small range of the parameters. Besides, as soon as they leave the shock, energy losses are so strong that they are thermalised within short distance.

4. Discussion

Figure 4 recapitulates the expected trend of the CR ionisation rate in different environments. Diffuse clouds and starless dense cores are well-characterised from both the observational and theoretical point of view even if, for starless cores, there are still uncertainties due to the complex chemical network, to the carbon depletion onto dust grains, and to the actual configuration of magnetic fields. Moving from the prestellar to the protostellar phase, one expects the ionisation degree to be fixed by short- and long-lived radioactive nuclei (^{26}Al and ^{40}K, respectively; Umebayashi and Nakano [44]) since interstellar CRs cannot penetrate close to the protostar. This is what we labelled *quiescent* phase in figure 4 as opposed to an *active* phase when strong shocks arise and conditions for the acceleration of local thermal particles to relativistic energies are verified.

In fact, equation 18 is highly non-linear: a variation in one or several parameters among shock velocity, temperature, magnetic field strength, ionisation fraction, and total hydrogen density can halt the acceleration process. For example, if requirements for acceleration are fulfilled, the ionisation rate can locally increase by orders of magnitude and the ionisation fraction can dramatically change. As a consequence the efficiency of the acceleration can be deeply altered. This is why we distinguish a quiescent from an active phase and we suppose a cyclic, intermittent acceleration rather than continuum.

5. Conclusions

In this paper we discussed the possibility of accelerating local thermal particles in a protostellar source turning them into CRs through the diffusive shock acceleration mechanism. We analysed three possible acceleration sites (accreting envelopes, jets, and protostellar surface) and we identified shocks along jets and on the surface of the

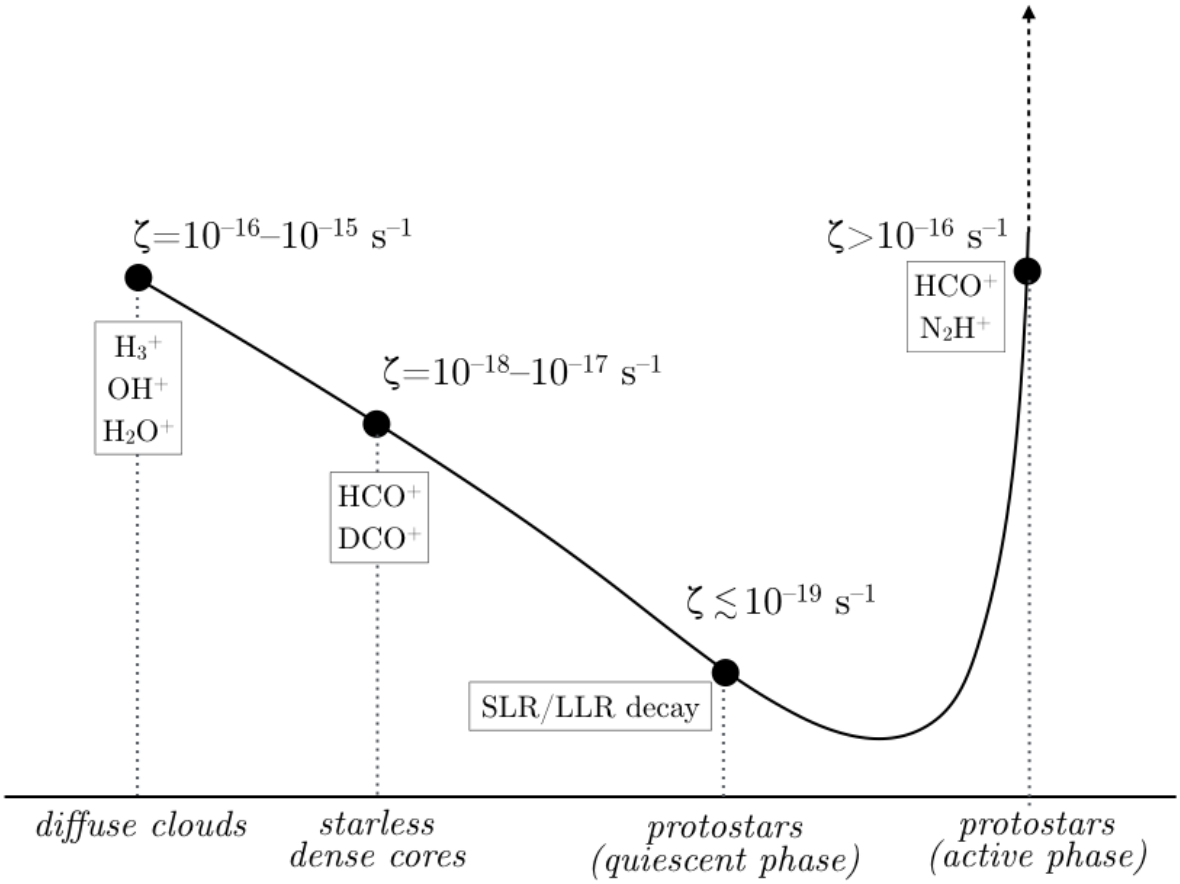

Figure 4. Values of the CR ionisation rate for different environments. Boxes show the molecular tracers that are usually used to estimate ζ except for the quiescent phase of protostars where SLR/LLR stands for short- and long-lived radioactive nuclei (see section 4 for details).

protostar to be the best candidates, while in envelopes the acceleration is quenched because shocks are sub-Alfvénic and ionisation fraction and shock velocity are too small. While thermal protons can be boosted up to energies of tens of GeV, thermal electrons reach MeV energies but only for a narrow combination of the parameters. Electrons are also quickly re-thermalised because of strong energy losses. In Padovani *et al* [34] we successfully applied this modelling to explain recent observations of high ionisation rate and synchrotron emission in protostars.

The main limiting factor to our study is related to uncertainties on the parameters determined by observations. For this reason, our modelling represents a proof of concept, in fact we assumed a constant value for all the parameters all along the shock front, while for instance shock velocities are usually larger at the shock apex and decrease along the wings. Further observations at higher resolution with new generation telescopes such as the Atacama Large Millimeter/Submillimeter Array (ALMA) will aid to have better constraints with a special consideration for the magnetic field configuration. In fact, being charged particles, CRs perform a spiral motion along magnetic field lines and the

knowledge of the magnetic structure is a key point for correctly applying the propagation models (e.g., Padovani and Galli [29]; Padovani *et al* [31]). As shown in figure 3, the most limiting condition on the maximum energy reached by a thermal proton in a jet shock is due to the jet geometry through the condition on $t_{\rm esc,d}$. In this work we focused on shocks in low-mass protostars at a distance of 100 AU from the central source, but in principle we can apply the same formalism to high-mass protostars that usually have larger shock velocity at larger distance from the source. Since $t_{\rm acc} \propto U^{-2}$ and $t_{\rm esc,d} \propto R_{\perp}^2$, thermal protons may be accelerated up to $1 - 10$ TeV and their γ emission could be observed by telescopes such as the High Energy Stereoscopic System (HESS) or the Cherenkov Telescope Array (CTA). Finally, low-frequency observations with the Giant Metrewave Radio Telescope (GMRT) and the Low-Frequency Array (LOFAR) can be used to search for synchrotron emission in low- and high-mass protostars, revealing the acceleration of local electrons. The synergy between molecular line observations and (sub-)millimetre observations will help in understanding how much the process of local CR acceleration is common during the star formation process **(see also Becker** *et al* **[4]; Schuppan** *et al* **[39] for the correlation between γ emission and ionisation).**

Acknowledgments

We want to thank the two referees for very helpful comments, which further improved the quality of this paper. This work has been carried out thanks to the support of the OCEVU Labex (ANR-11-LABX-0060) and the A*MIDEX project (ANR-11-IDEX-0001-02) funded by the "Investissements d'Avenir" French government programme managed by the ANR.

References

[1] Abdo A A *et al* 2010, *ApJ*, **723**, 649
[2] Ainsworth R E, Scaife A M M, Ray T P, Taylor A M, Green D A and Buckle J V 2014, *ApJ*, **792**, 18
[3] Araudo A T, Romero G E, Bosch-Ramon V and Paredes J M 2007, *A&A*, **476**, 1289
[4] Becker J K, Black J H, Safarzadeh M and Schuppan F 2011, *ApJ*, **739**, 43
[5] Berezhko E G & Ellison D C 1999, *ApJ*, **526**, 385
[6] Bosch-Ramon V, Romero G E, Araudo A T and Paredes J M 2010, *A&A*, **511**, A8
[7] Caselli P, Walmsley C M, Terzieva R and Herbst E 1998, *ApJ*, **499**, 234
[8] Ceccarelli C, Dominik C, López-Sepulcre A, Kama M, Padovani M, Caux E and Caselli P 2014, *ApJL*, **790**, 1
[9] Cecchi-Pestellini C and Aiello S, 1992, *MNRAS*, **258**, 125
[10] de Gouveia Dal Pino E M 1995, *AIPC*, **345**, 427
[11] de Gouveia Dal Pino E M and Lazarian A 2005, *A&A*, **441**, 845
[12] Desch S J, Connolly H C Jr and Srinivasan G 2004, *ApJ*, **602**, 528
[13] Drury L O'C, 1983, *RPPh*, **46**, 973
[14] Drury L O'C, Duffy P and Kirk J G 1996, **A&A**, **309**, 1002
[15] Ferrière K 2001, *RvMP*, **73**, 1031

[16] Ferris J P, Joshi P C, Edelson E H and Lawless J G 1978, *J. Mol. Evol.*, **11**, 293
[17] Galli D and Padovani M CRISM 2014 proceedings
`http://adsabs.harvard.edu/abs/2015arXiv150203380G`
[18] Giacalone J and Jokipii J R 2007, *ApJ*, **663**, 41
[19] Glassgold A E, Galli D and Padovani M 2012, *ApJ*, **756**, 157
[20] Grenier I A, Black J H and Strong A W 2015, *ARA&A*, **53**, 199
[21] Indriolo N and McCall B J 2012, *ApJ*, **745**, 91
[22] Ivlev A, Padovani M, Galli D and Caselli P 2015, *ApJ*, **812**, 135
[23] Kirk, J G 1994, in *Plasma Astrophysics*, ed. A O Benz and T J-L Courvoisier (Springer Verlag, Berlin), **225**
[24] Kulsrud R and Cesarsky C J 1971, *ApL*, **8**, 189
[25] Masunaga H and Inutsuka S 2000, *ApJ*, **531**, 350
[26] Munar-Adrover P, Paredes J M and Romero G E 2011, *A&A*, **530**, A72
[27] Neufeld D A *et al* 2010, *A&A*, **518**, L108
[28] Padovani M, Galli D and Glassgold A E 2009, *A&A*, **501**, 619
[29] Padovani M and Galli D 2011, *A&A*, **530**, A109
[30] Padovani M and Galli D 2013, in *Advances in Solid State Physics, Cosmic Rays in Star-Forming Environments*, ed. D F Torres and O Reimer, **34**
[31] Padovani M, Hennebelle P and Galli D 2013, *A&A*, **560**, A114
[32] Padovani M, Galli D, Hennebelle P, Commerçon B and Joos M 2014, *A&A*, **571**, A33
[33] Padovani M, Hennebelle P, Marcowith A and Ferrière K 2015, *A&A*, **582**, L13
[34] Padovani M, Marcowith A, Hennebelle P and Ferrière K 2016, *A&A*, **590**, A8
[35] Podio L, Lefloch B, Ceccarelli C, Codella C and Bachiller R 2014, *A&A*, **556**, A64
[36] Prantzos N *et al* 2011, *Rev. Mod. Phys.*, **83**, 1001
[37] Prasad S S and Tarafdar S P 1983, *ApJ*, **267**, 603
[38] Rieger F M and Duffy P 2006, *ApJ*, **652**, 1044
[39] Schuppan F, Becker J K, Black J H and Casanova S 2012, *A&A*, **541**, A126
[40] Shu F H, Adams F C and Lizano S, 1987, *ARA&A*, **25**, 23
[41] Shu F H, Galli D, Lizano S and Cai M 2006, *ApJ*, **647**, 382
[42] Stone E C, Cummings A C, McDonald F B, Heikkila B C, Lal, N and Webber, W R 2013, *Science*, **341**, 150
[43] Tavani M *et al* 2009, *ApJ*, **698**, L142
[44] Umebayashi T and Nakano T 2009, *ApJ*, **690**, 69
[45] Vaupré S, Hily-Blant P, Ceccarelli C, Dubus G, Gabici S and Montmerle T 2014, *A&A*, **568**, A50

Table 1. Parameters to compute the maximum energy reached by a thermal proton for a parallel shock in the Bohm regime ($\kappa_{\rm u} = \kappa_{\rm B}$) and a shock efficiency $\eta = 10^{-5}$.

Model	U [km s^{-1}]	B [G]	$n_{\rm H}$ [cm^{-3}]	x	T [10^4 K]	$R_{\rm sh}$ [AU]	$R_\perp$ [AU]	$E_{\rm max}$ [GeV]
$\mathcal{W}$	40	5×10^{-5}	10^5	0.33	1	100	10	0.13
$\mathcal{S}$	160	10^{-3}	6×10^5	0.60	1	100	10	12.9
$\mathcal{P}$	260	5	1.9×10^{12}	0.30	94	2×10^{-2}	–	27.2